

EML RESEARCH REPORT NO. 4

PARAMETRIC STUDY OF OVERSIZED
RECTANGULAR WAVEGUIDES AND H-GUIDES

F. J. Tischer

This research was supported by
The National Aeronautics and Space Administration
and partially funded under NGR-34-002-047

NORTH CAROLINA STATE UNIVERSITY .

Raleigh, North Carolina

December 1966

GPO PRICE \$ _____

CFSTI PRICE(S) \$ _____

Hard copy (HC) ~~8.00~~

Microfiche (MF) ~~2.00~~

ff 653 July 65

N67 18048

FACILITY FORM 502

(ACCESSION NUMBER)
23
(PAGES)

CK81 710
(NASA CR OR TMX OR AD NUMBER)

(THRU)
X 0
(CODE)
09
(CATEGORY)

PARAMETRIC STUDY OF OVERSIZED
RECTANGULAR WAVEGUIDES AND H-GUIDES

by F. J. Tischer

ABSTRACT

The effects of the cross-sectional geometry on the attenuation due to wall losses of oversized rectangular waveguides and H-guides is considered. By properly chosen normalizations, the dependence on width, height, oversize ratio A^2/λ^2 and aspect ratio a/b are determined, optimum geometries found, and the data displayed in diagram form. The attenuation of an H-guide with infinitely thin dielectric slab with infinite permittivity is compared with that of the parallel-wall guide as reference. It is found that the dielectric slab reduces the attenuation due to wall losses by a factor depending primarily on the rate of the exponential decay of the fields in the air space. The approach of derivation permits showing clearly the causes of the decreased attenuation.

CONTENTS

I.	Introduction	Page 1
II.	General Relationships	2
III.	First Type of Normalization	4
IV.	Minimization of Attenuation	6
V.	H-guide with zero-thickness dielectric slab	7
VI.	Comparison of H-guide attenuation	11
VII.	Conclusions	13
VIII.	References	14

I. INTRODUCTION

The application of oversized waveguides in the millimeter-wave region offers attractive solutions of problems of energy transmission and circuit design in this frequency range. Oversized waveguides, in contrast to standard-size guides have considerably reduced attenuation, high power carrying capability before breakdown, and cross-sectional sizes suitably augmented for practical design. The simultaneous transmission of higher-order modes on the other hand represents a disadvantage which, due to a lack of experience in design and operation of practical systems cannot be properly assessed. Careful design and application of mode filters are expected to eliminate major effects of higher order modes.

It is the objective of this paper to present results of a study of minimizing the attenuation due to wall losses of oversized waveguides. Rectangular waveguides with TE waves and H-guides excited in the low-loss hybrid mode are considered. There exists a considerable amount of literature on the attenuation of waveguides with the publications dealing mostly with standard-size waveguides carrying the fundamental mode (1-9), with the frequency dependence of the attenuation (1, 3, 8, 9), with the various modes which can be excited, and with their cutoff frequencies (4, 8, 9). In the present paper emphasis is placed on showing how the cross-sectional geometry affects the attenuation of oversized guides at a given frequency. The results show what geometry gives minimum attenuation.

As a first step, general dependences of the attenuation on the dimensions are considered; then the normalization is changed to permit optimization. An oversize ratio $OSR = A^2/\lambda^2$ given by the ratio of cross-sectional area divided by the square of the operational wavelength is introduced as a basis

for the optimization. The attenuation of the H-guide is considered next under assumption of an infinitely thin dielectric slab with the cross-sectional distribution of the permittivity in the form of a Dirac delta function.

II. GENERAL RELATIONSHIPS

The attenuation of waveguides with arbitrary cross-section due to wall losses can be derived from the field distribution computed under assumption of perfectly conducting walls. At millimeter waves the relationships become more complicated due to the effects of the structure of the surfaces as shown in the literature (6). These effects will be disregarded in the present analysis. The attenuation is usually derived from the magnetic field intensities adjacent to the conducting walls which in combination with the surface resistance yield the dissipated power per unit length and from the cross-sectional distribution of its transverse component which gives the power carried by the waves along the guide. The corresponding equation for transverse electric (TE) waves is (2)

$$\alpha = \frac{R_s}{2kk_zZ} \frac{k_z^2 \int_D \left[\frac{dH_z}{ds} \right]^2 ds + (k^2 - k_z^2) \int_C H_z^2 ds}{\int_A (\nabla_t H_z)^2 dA}, \quad (1)$$

where H_z is the longitudinal component of the magnetic field intensity, $\nabla_t H_z$ and its transverse gradient, k and z are the propagation constant and impedance of plane waves in the medium of the guide, k_z the guide wavelength, and R_s is the surface resistance. The latter is related to the skin depth and given by

$$R_s = \sqrt{\frac{\omega\mu}{2\sigma}} = \left[4.52 \times 10^{-2} \frac{1}{\lambda[\text{cm}]} \right]_{\text{copper}}. \quad (2)$$

The quantities in this equation are the operational frequency ω , the permeability μ , the conductivity σ , and the wavelength λ . The integrations in Eq. (1)

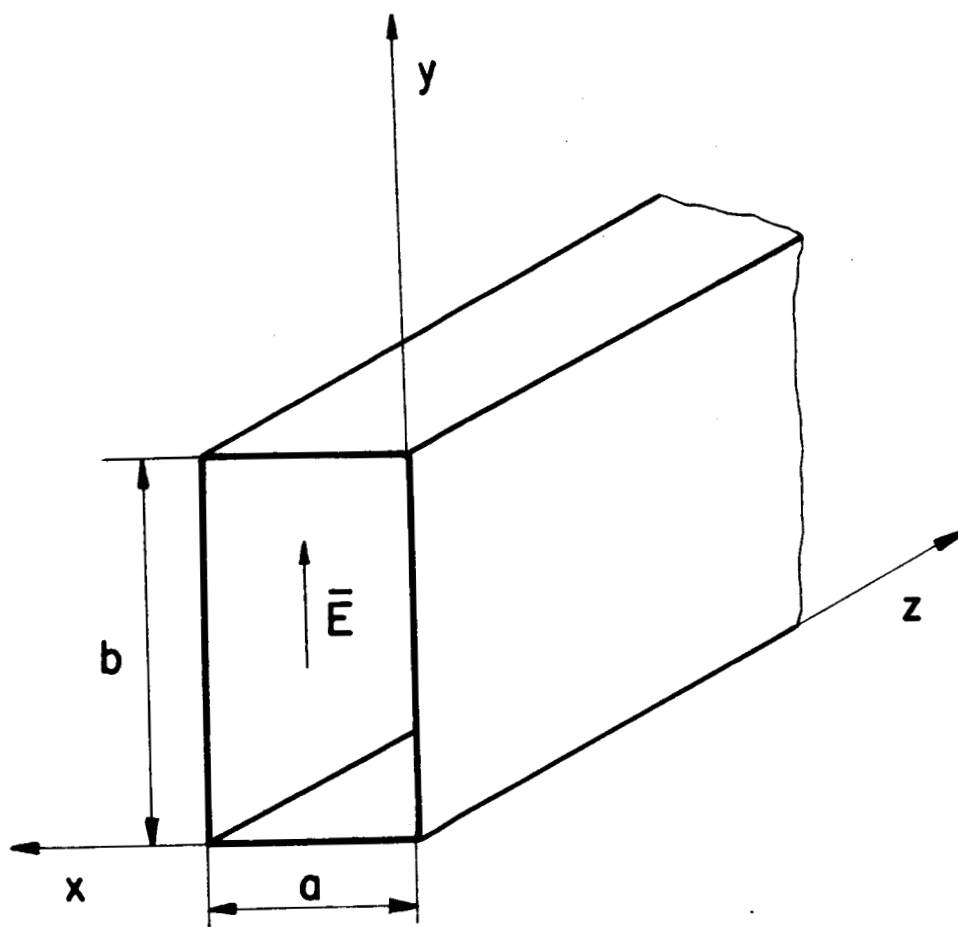


Fig.1. Geometry of the oversized waveguide.

are carried out along the boundary C and over the cross-section A .

For a rectangular waveguide with its geometry shown in Fig. 1, the attenuation constant becomes

$$\alpha = \frac{2 R_s}{Z k k_z} \left[\left(\frac{m \pi}{a} \right)^2 \frac{1}{a} + \frac{1}{2b} k^2 \right]. \quad (3)$$

The derivation shows that the first term in the brackets is the result of the longitudinal component H_z only while the second term results from both, the longitudinal and transverse components. This is confirmed if we let a and b alternatively approach infinity. If $a \rightarrow \infty$, we obtain a parallel-strip line with TEM waves and with only a transverse component of the magnetic field intensity. The electric field intensity vector stands perpendicular to the walls. The attenuation becomes

$$a \rightarrow \infty : \quad \alpha_{\parallel} = \frac{R_s}{Z b} \quad (4a)$$

We observe that the attenuation increases with the square root of the frequency due to the frequency dependence of R_s .

If b approaches infinity, the attenuation is

$$b \rightarrow \infty : \quad \alpha_{\parallel} = \frac{2 R_s}{Z k k_x} \left(\frac{m \pi}{a} \right)^2 \frac{1}{a} \quad (4b)$$

The guide is now a parallel-strip line with the electric field vector parallel to the walls and the longitudinal component of the magnetic field intensity contributing to the wall losses. Transformed into a more convenient form, the equation becomes for $m=1$

$$\alpha_{\parallel} = \frac{R_s}{Z a} \frac{(\lambda/a)^2}{\sqrt{1 - (\lambda/a)^2/4}} \quad (5)$$

where the second fraction represents a factor which indicates the change of the attenuation if the field configuration is changed in a parallel-strip line from

TEM waves (Eq. 4a) to TE waves with E parallel to the walls. We observe that the attenuation now decreases with $1/f^{3/2}$ and that oversize conditions of spacing between the walls reduces the attenuation considerably more than in the former case of TEM waves when E was perpendicular to the walls. Comparison with the low-loss wave mode TE_{10} for the circular guide shows that the frequency dependence of the attenuation in both cases is the same.

FIRST TYPE OF NORMALIZATION

In this section the attenuation according to Eq. (3) is considered in detail for finding how increases of the dimensions alternatively in the x and y direction affect its magnitude. Two parameters $\xi = \lambda/a$ and $\eta = \lambda/b$ are introduced which are inverse proportional to the width and height respectively and normalized with respect to λ . Equation (3) is then modified accordingly to show the dependences on these parameters. We find

$$\alpha' = \frac{\eta + 2\left(\frac{m}{2}\right)^2 \xi^3}{\sqrt{1 - \left(\frac{m}{2}\right)^2 \xi^2}}, \quad (6)$$

where

$$\alpha' = \alpha \lambda^{3/2} \sqrt{Z_0/\pi}.$$

The resulting relationships are illustrated graphically in Fig. 2. The diagram shows the normalized attenuation α' as a function of ξ with the mode number m as parameter for 4 values of η which indicate the height. The attenuation approaches terminal values for increasing width ($\xi \rightarrow 0$) which represent the attenuation of the parallel-strip line with TEM waves. For decreasing width (increasing ξ), the attenuation increases steadily and approaches infinity at cutoff when the denominator goes to zero. The second term in the numerator of Eq. (6) is responsible for the basic dependence of α' on ξ .

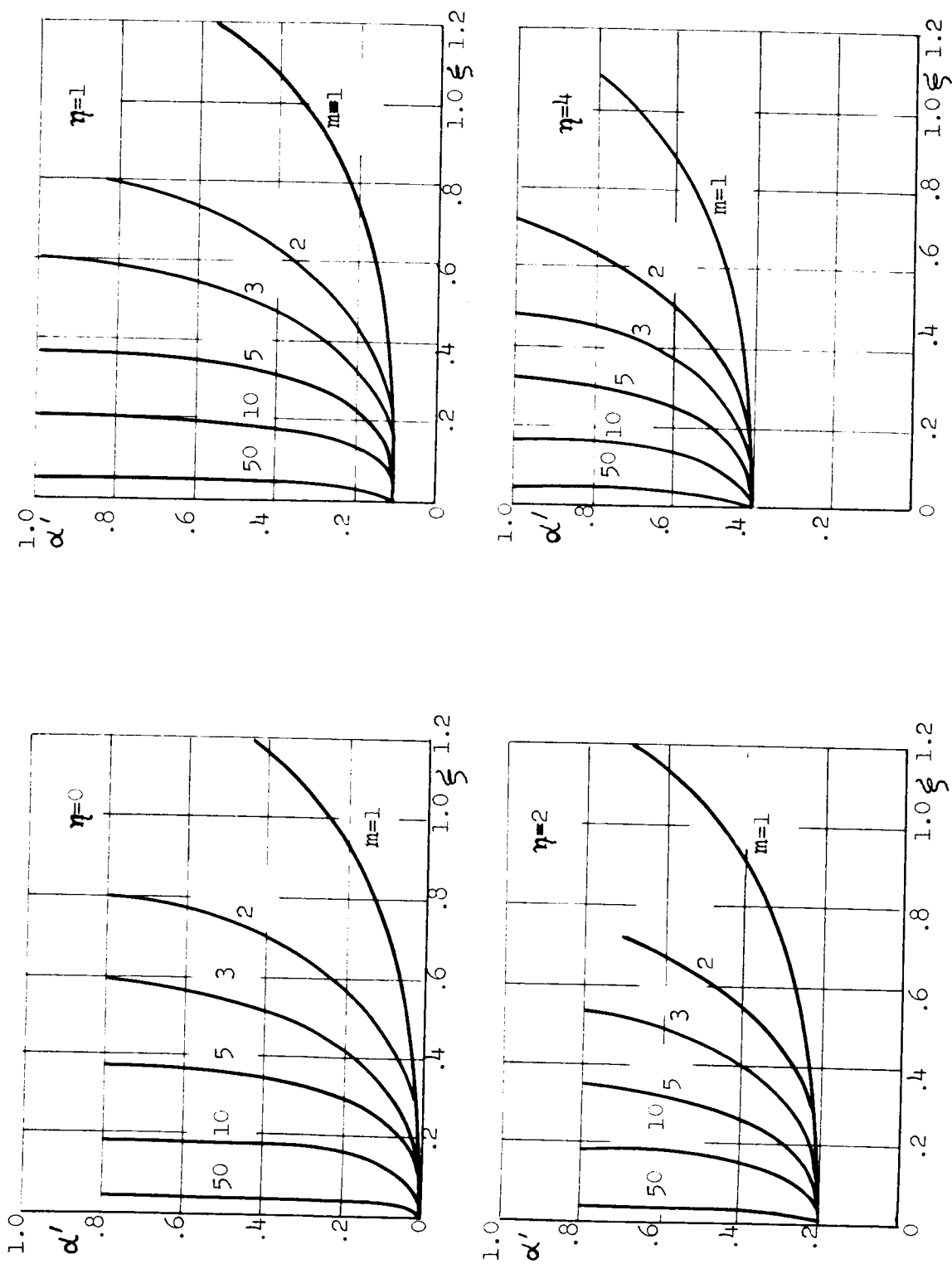


Fig. 2. Normalized attenuation as a function of width of the guide a ($\xi = \lambda/a$).

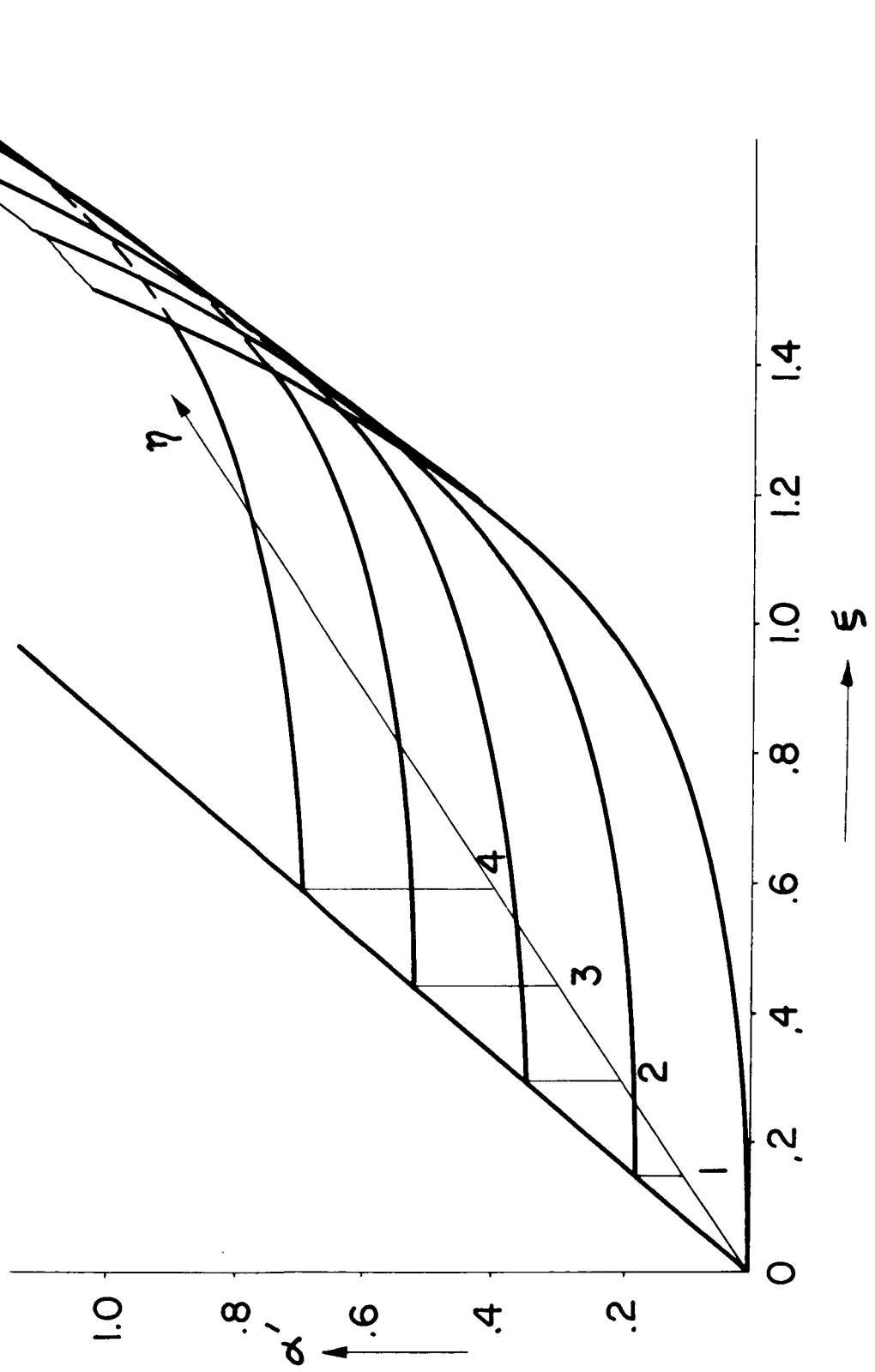


Fig. 3. Normalized attenuation as a function of width and height.
 $[\xi = \lambda/a, \eta = \lambda/b, \alpha' = \alpha \lambda^{3/2} (2\sigma/\pi)^{1/2}]$.

The attenuation increases with increasing mode number of the higher-order waves reaching very large values near cutoff of each one. This may be an advantage for loose mode coupling since it may reduce resonance effects involving higher-order modes. It may cause on the other hand considerable transmission losses in the case of strong coupling. Mode-coupling effects are hence very important in oversized waveguides.

The dependence on the height of the guide is given by the linear relationship with η expressed by the first term in the numerator of Eq. (6), which in the diagrams causes α' to move upward toward higher values. With increasing height, η approaches zero and α' assumes a limiting value which corresponds to the attenuation of the parallel strip line with the E field parallel to the walls.

The relationships can be instructively illustrated by three-dimensional diagrams for which Fig. 3 shows an example for $m=1$. The attenuation is indicated by a surface where the vertical distance of each point from the $\xi\eta$ -plane indicates α' as a function of ξ and η . Such surfaces can be determined for each wave number representing one wave mode. Lines of constant attenuation can also be inserted which additionally illustrate the shape of the surface. The basic shape suggests that it seems possible to minimize the attenuation after choosing a suitable quantity as basis for the optimization. Such a quantity is a constant product of ξ, η which is the ratio of the wavelength squared divided by the cross-sectional area. This quantity represents a measure for the oversize dimensions of the guide and its reciprocal value will be called "oversize ratio" (OSR). In the diagram of Fig. 3, the corresponding attenuation is found on the surface for a particular value of m as the intersection with a vertical cylinder given by $\xi\eta = \text{constant}$.

MINIMIZATION OF ATTENUATION

A second type of modification of Eq. (3) which permits optimization of the attenuation is based on introduction of the previously discussed oversize ratio. The following substitutions are made,

$$p = (m/2)^2 (\lambda^2/A),$$

$$q = a/b.$$

The first parameter contains the oversize ratio, $OSR = A^2/\lambda^2$, and the mode number m ; the second is the aspect ratio, where $q > 1$ indicates a wide guide with low height and $q < 1$ a narrow tall guide.

Substitution into Eq.(3) yields a normalized attenuation

$$\alpha'' = \sqrt{pq} \frac{1 + 2p/q^2}{\sqrt{1 - p/q}}, \quad (7a)$$

which is related to the actual attenuation α by

$$\alpha = \alpha'' \frac{2R_s}{2\lambda m} \quad (7b)$$

For a given wave mode, α'' depends on the oversize ratio and geometry only. The relationships of Eq. (7a) are shown in diagram form in Fig. 4 for a wide range of the parameter p . The diagram indicates that the attenuation can be minimized requiring a different optimum aspect ratio for each value of the oversize ratio and mode number.

The minimization by differentiation leads to

$$\frac{d\alpha''}{dq} = [] [q^3 - 2pq^2 - 6pq + 4p^2]$$

and to

$$q^3 - 2pq^2 - 6pq + 4p^2 = 0. \quad (8)$$

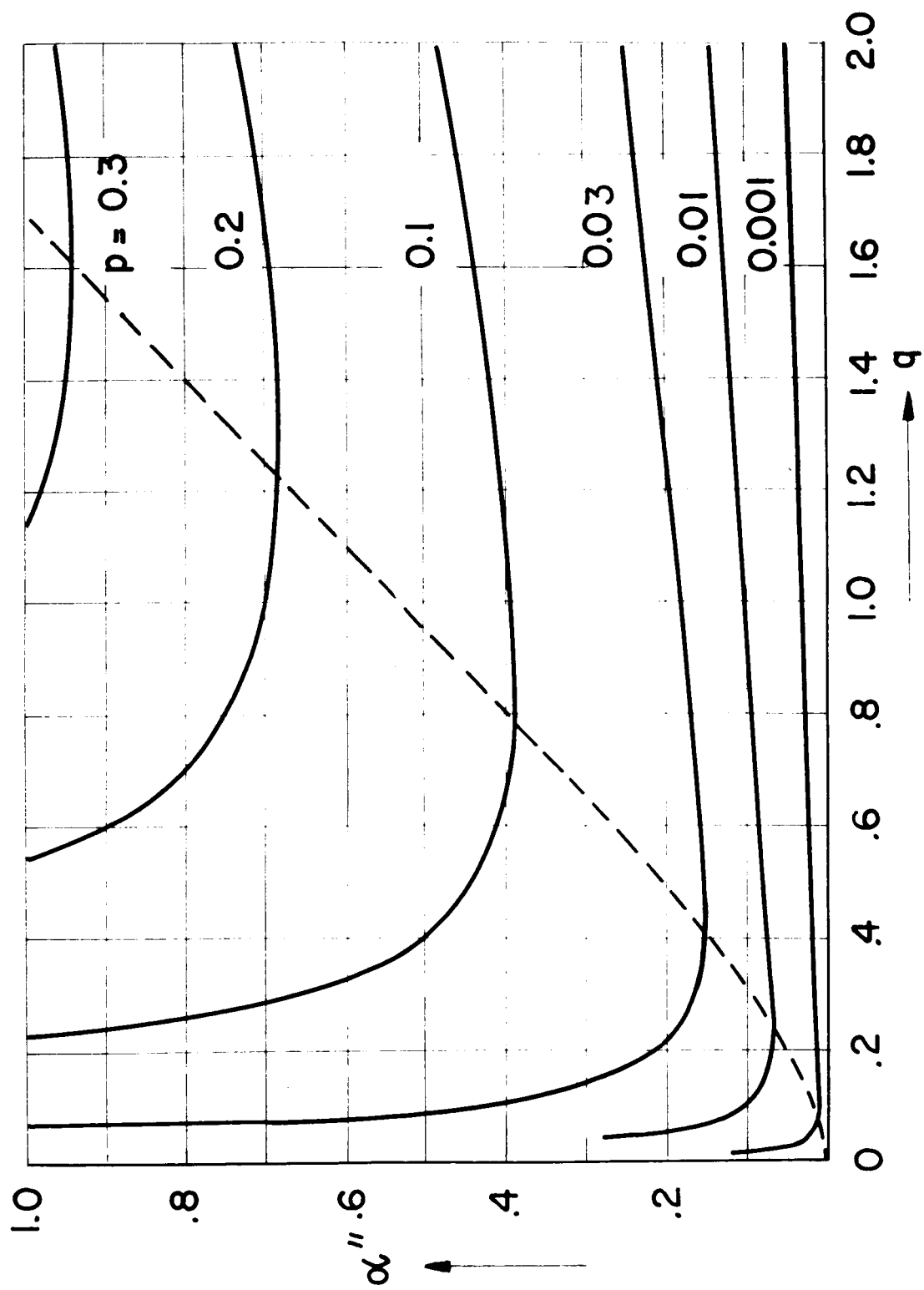


Fig. 4. Normalized attenuation depending on aspect ratio and OSR.

For large values of oversize ratio, a simple approximation can be obtained

$$A \gg \lambda^2 : \left[\left(\frac{b}{a} \right)^2 \right]_{\alpha' = \min} \approx \frac{2}{3} \frac{A}{m^2 \lambda^2} \quad (9)$$

which gives the following equation for the optimized attenuation of oversized waveguides,

$$\alpha_{\min} \approx \frac{R_s}{Z \lambda_m} 2.09 p^{3/4}. \quad (10)$$

For more accurate computations, Eq. (8) can be simply solved for p in terms of q .

The results indicated in Fig. 4 show that the minima of the attenuation are comparatively shallow and that no drastic changes of the attenuation are caused by changes of the aspect ratio toward greater width of the guide. The effects of such changes become more pronounced, however, at increased oversize ratios by increasing the cross-sectional area of the guide. Considering higher-order wave modes, we observe that the minimum attenuation increases with increasing mode number.

H-GUIDE WITH ZERO - THICKNESS

DIELECTRIC SLAB

Studies of the H-guide and groove guide have shown that these guides have notably reduced attenuation in comparison with the rectangular standard guide with equal width. This raises the question whether this is also true in the case of oversize waveguides. Particularly interesting and important is the following more specific question: If we have a parallel-wall guide of given oversize width, disregard the upper and lower openings, and compare its attenuation due to wall losses with that of an oversized H-guide with equal width disregarding again the upper and lower openings and the dielectric losses, how do the values of attenuation compare. If they are equal, the application

of the H-guide concept offers no advantage under oversize conditions. If the H-guide has reduced attenuation, further studies of such guides and groove guides are necessary for determining their characteristics under these conditions.

A useful approach for the comparison consists of assuming an H-guide with an infinitely thin dielectric slab where the permittivity distribution in direction parallel to the walls follows a Dirac delta function. This eliminates the problem of the dielectric, the fields are primarily concentrated in the air space and an instructive comparison with the parallel-wall guide becomes possible. Figure 5 shows the compared structures.

The field distribution in the H-guide with zero-thickness slab has to be determined first; this is done by determining the fields of plane waves traveling along an infinite dielectric slab and by the subsequent insertion of the vertical walls which then form the actual guide.

The field distribution in air for PM waves (5,9) ("PM" indicates that the magnetic field vector is parallel to the dielectric slab) is found from Maxwell's equations and given by

$$\begin{aligned} E_t &= -\frac{k_z}{\omega \epsilon_0} H_0' e^{-\alpha_y y} e^{-jk_z s}, \\ E_e &= -j \frac{\alpha_y}{\omega \epsilon_0} H_0' e^{-\alpha_y y} e^{-jk_z s}, \\ H_t &= H_0' e^{-\alpha_y y} e^{-jk_z s}, \end{aligned} \quad (11)$$

The subscripts t and l indicate transverse and longitudinal components of the fields respectively. The propagation constant in the direction of wave propagation (s-direction) is k_z and the exponential decrease of the fields above and below the infinite slab in nepers per meter is denoted by α_y . The field components within the dielectric can be described correspondingly; they are of minor importance in the present case. Taking into account the boundary conditions on the surfaces of the slab yields for the wave parameters

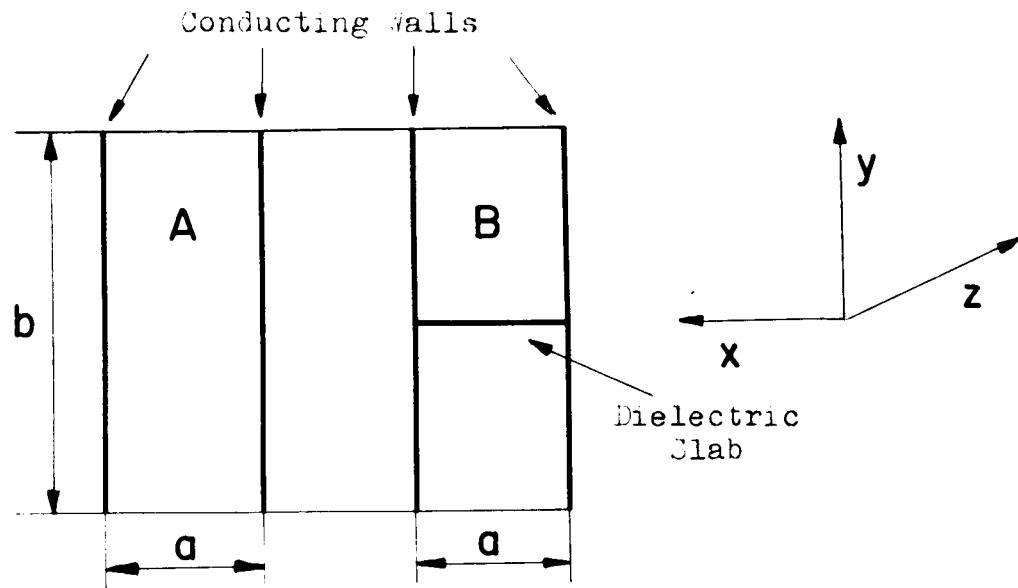


Fig.5. Cross-sections of compared guides.

A: Parallel-wall guide.

B: H-guide, zero-thickness slab.

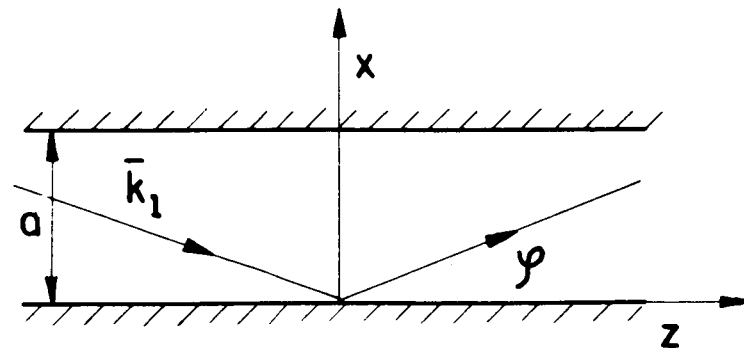


Fig.6. Geometry of wave reflections
in the H-guide.

$$\alpha_y = \frac{k_y}{\epsilon_r} \tan k_y \frac{D}{2}, \quad (11a)$$

$$k_0^2 \epsilon_r = k_y^2 + k_z^2, \quad (11b)$$

$$k_0^2 = -\alpha_y^2 + k_z^2, \quad (11c)$$

where ϵ_r and k_y are the relative permittivity and the propagation constant in the y-direction in the slab respectively, D is the thickness of the slab, and k_0 the phase constant of plane waves in air.

If we let ϵ_r become very large and approach infinity, we find from Eqs. (11)

$$\epsilon_r \rightarrow \infty : k_y^2 \approx k_0^2 \epsilon_r \rightarrow \infty \quad (12a)$$

$$D \approx \frac{\lambda_0}{2\sqrt{\epsilon_r}} \rightarrow 0 \quad (12b)$$

$$k_y \frac{D}{2} \approx \frac{\pi}{2}. \quad (12c)$$

We observe that α_y and k_z are indefinite, remain finite, and are interrelated by Eq. (11c). We also observe that the Eqs.(10) are basically not affected by the transition to an infinitely thin slab and remain the same.

At the next step, the slab is placed between two conducting walls a distance "a" apart. The waves are reflected between the walls with the geometry indicated in Fig. 6. Superposition of the waves reflected under an angle ϕ between the walls yield then the field distribution in the corresponding H-guide. We find

$$\begin{aligned} H_z &= H_0 \cos k_x x e^{-\alpha_y y} e^{-jk_z z}, \\ H_x &= j \frac{k_z}{k_x} H_0 \sin k_x x e^{-\alpha_y y} e^{-jk_z z}, \\ E_z &= \frac{\alpha_y}{\omega \epsilon_0} \frac{k_z}{k_x} H_0 \sin k_x x e^{-\alpha_y y} e^{-jk_z z}, \\ E_x &= j \frac{\alpha_y}{\omega \epsilon_0} H_0 \cos k_x x e^{-\alpha_y y} e^{-jk_z z}, \\ E_y &= -j \frac{k_z^2}{\omega \epsilon_0 k_x} H_0 \sin k_x x e^{-\alpha_y y} e^{-jk_z z}, \\ H_0 &= -2 \frac{k_x}{k_z} H_0', \end{aligned} \quad (13)$$

and

$$k_z^2 = k_x^2 + k_y^2, \quad (14)$$

$$k_x = m\pi/a, \quad (15)$$

The resulting equations contain α_y and k_z but are otherwise independent of the thickness of the slab. For zero-thickness and infinite ϵ_r these quantities can have any value as long as Eqs. (11c) and (14) are satisfied. Combination of these equations yields

$$\alpha_y^2 = k_x^2 + k_z^2 - k_0^2. \quad (16)$$

The exponential decay factor α_y will be used henceforth for the description of the propagation characteristics of the H-guide.

We observe that the H-guide becomes a parallel-wall guide as α_y approaches zero and that the guide wavelength assumes under this condition the well known form

$$\alpha_y = 0 \quad k_{z0} = (k_0^2 - k_x^2)^{1/2},$$

so that

$$\alpha_y^2 = k_z^2 - k_{z0}^2. \quad (17)$$

The attenuation of the H-guide is obtained by the equation

$$\alpha_H = p_{\text{diss}} / 2 p_{\text{trans}}$$

from the power dissipated in the walls per unit length in a section per unit height (p_{diss}) and from the power carried by the waves in the same section of the guide. Since all field components decrease exponentially with α_y in the y-direction, the attenuation becomes independent of the integration in this direction and the attenuation of a section per unit height becomes representative of the whole guide. Insertion of the field intensities into the equations for p_{diss} and p_{trans} ,

$$p_{\text{diss}} = R_s [H_z^2]_{x=0},$$

$$p_{\text{trans}} = -\frac{1}{2} \int_0^a E_y H_x^* dx,$$

yields finally

$$\alpha_H = \frac{2R_s}{2a} \frac{k_0}{k_z} \frac{k_x^2}{k_x^2 + k_z^2}. \quad (19)$$

It should be noted that the derived equation for α_H can also be used for rough estimates of the attenuation in oversized groove guides for $q \ll 1$ where the energy transport occurs mainly in the upper and lower parallel-wall sections of the guide.

COMPARISON OF H-GUIDE ATTENUATION

For comparing the attenuation of the zero-thickness H-guide with that of other guides it is practical to compare it first with that of the parallel-wall guide as an intermediate step. This guide can be used as a reference and the attenuation of other guides referred to that of this guide.

The attenuation of the H-guide given by Eq.(19) can be transformed into that of the parallel-wall guide by letting α_y approach zero. Under this condition k_z becomes k_{z0} according to Eq.(17) and we obtain

$$\alpha_{||} = \frac{2R_s}{Z_0} \frac{k_0}{k_{z0}} \frac{k_x^2}{k_0^2}. \quad (20)$$

Substitution of k_z according to Eq.(17) into (19) yields a modification of this equation in the form

$$\alpha_H = \alpha_{||} \left[1 + (\alpha_y / k_{z0})^2 \right]^{-1/2} \left[1 + (\alpha_y / k_0)^2 \right]^{-1}, \quad (21)$$

where it is expressed in terms of $\alpha_{||}$ multiplied by a factor which depends on the characteristics of the H-guide. These can be described by the two parameters

$$p = \frac{\alpha_y}{k_0} \quad \text{and} \quad q = \frac{k_0}{k_{z0}},$$

so that

$$\alpha_H = \alpha_{||} F(p, q);$$

$$F(p, q) = (1 + p^2 q^2)^{-1/2} (1 + p^2)^{-1},$$

where $F(p,q)$ by structure of the equation indicates a reduction of the attenuation which is caused by the effects of the dielectric slab which transforms the parallel-wall guide into an H-guide.

The result is important since it contradicts the sometimes heard statement that the attenuations due to wall losses of both, H-guide and parallel-wall guide, are equal.

The reason for the decreased attenuation can be seen by inspection of Eqs(10) and (13). We observe that introduction of the dielectric slab along the propagation path of plane waves introduces a longitudinal electric field component E_z (Eqs.(10)) which in the case of the H-guide becomes the component E_z , this additional longitudinal field component can be considered as the origin of TM waves not present in the parallel-wall guide which carry additional power along the guide without contributing to the wall losses. These are caused by the longitudinal component of the magnetic field intensity H_z which is related to TE waves only. They remain, from a viewpoint of a direct relationship unaffected by the introduction of the dielectric slab.

The reduction factor $F(p,q)$ is shown graphically in Fig. 7 as a function of p with q as parameter. The parameter p may vary between zero and one for practical H-guides and q exceeds one depending on the width of the guide and wavelength.

Considering now the attenuation of the oversized H-guide more generally, the fact that it is smaller than that of the parallel-wall guide indicates that it is considerably below that of the oversized rectangular waveguide where the upper and lower walls contribute to additional losses and to increased attenuation. It should be noted, however, that the dielectric losses in the slab were disregarded in an attempt to derive basic relationships. These losses may offset the improvements by the basic field structure. Further trade-off studies are necessary for determining the conditions under which this occurs.

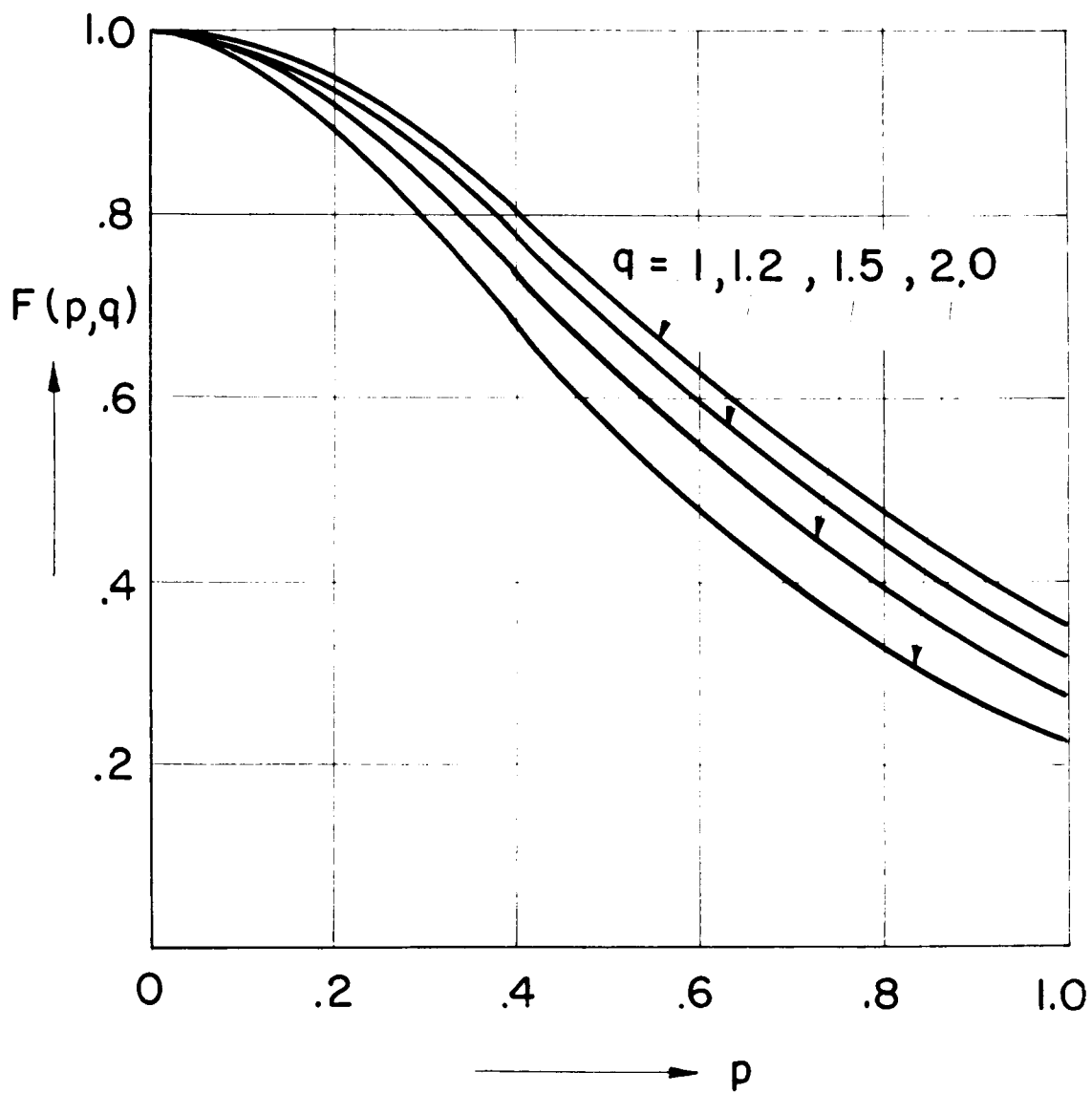


Fig.7. Reduction factor of attenuation due to reduced guide wavelength in the H-guide.

CONCLUSIONS

In the present paper appropriate normalizations were chosen to show the effects of the geometry on the attenuation of oversized rectangular waveguides and H-guides. One set of parameters in the equation of attenuation for the rectangular guide has shown clearly the dependence on width and height where infinitely extended parallel-wall guides were the limiting cases. Introduction of an oversize ratio, $OSR = A/\lambda^2$, and of the aspect ratio yields another modified equation which shows that the attenuation can be minimized and allows determination of the optimum geometry. Diagrams based on these normalized equations show instructively the effects of geometry changes and the influence of oversize dimensions.

The H-guide was considered under assumption of an infinitely thin dielectric slab with infinite permittivity. This approach allows a basic comparison of its attenuation with that of the parallel-wall guide as a reference value. This can be in turn compared with the values of oversized rectangular waveguides considered in the preceding sections. The result is important since it clearly states that the attenuation due to wall losses of the H-guide is lower than that of the parallel-wall guide. Consequently it is additionally lower than that of the oversized rectangular guide. It should be noted that the dielectric losses in the slab were neglected which cause an increase of the attenuation. More detailed studies are required for showing optimum geometries including the dielectric losses.

REFERENCES

- (1) Kuhn, S.: "Calculation of Attenuation in Wave Guides." J. Inst. Elec. Eng., 1946, 93, Part III A, 663-678.
- (2) Collin, E. R.: "Field Theory of Guided Waves." McGraw-Hill Book Co., Inc., New York, 1960.
- (3) Tischer, F. J.: "A Waveguide Structure with Low Losses." Arch. Elekt. Übertragung, 1953, 7, 592-596.
- (4) Tischer, F. J.: "Properties of the H-Guide at Microwave and Millimeter Waves." 1956 IRE Convention Record, Pt. 5, 44-51.
- (5) Cohn, M.: "Propagation in a Dielectric-Loaded Parallel Plane Waveguide." IRE Transactions, 1959, Vol. MTT-7, 202-208.
- (6) Benson, F. A. and Steven, D. H.: "Rectangular-Waveguide Attenuation at Millimeter Wavelength." Proc. IEE, 1963, 110, 1008-1014.
- (7) Tischer, F. J.: "The Groove Guide, a Low-Loss Waveguide for Millimeter Waves." IEEE Transactions, Vol. MTT-11, 1963, 291-296.
- (8) Griemsmann, J.W.: "Oversized Waveguides." Microwaves, 1963, 2, 20-23.
- (9) Benson, F. A. and Conlon, R.F.B.: "Propagation and Attenuation in the Double-Strip H-Guide." Proc. IEE, 1966, 113, 1311-1320.